Conditional over-expression of PITX1 causes skeletal muscle dystrophy in mice

Sachchida N. Pandey[1,*], Jennifer Cabotage[1,*], Rongye Shi[1], Manjusha Dixit[1], Margret Sutherland[2,3], Jian Liu[4], Stephanie Muger[3], Scott Q. Harper[4,5], Kanneboyina Nagaraju[1,2] and Yi-Wen Chen[1,2,‡]

[1]Center for Genetic Medicine Research, Children's National Medical Center, Washington, DC 20010, USA
[2]Department of Integrative Systems Biology, George Washington University, Washington, DC 48109, USA
[3]Center for Neuroscience Research, Children's National Medical Center, Washington, DC 20010, USA
[4]Center for Gene Therapy, The Research Institute at Nationwide Children's Hospital, Columbus, OH 43205, USA
[5]Department of Pediatrics, Ohio State University College of Medicine, Columbus, OH 43205, USA

*These authors contributed equally to this work
‡Author for correspondence (ychen@cnmcresearch.org)

Biology Open 1, 629–639
doi: 10.1242/bio.20121305
Received 13th March 2012
Accepted 26th April 2012

Summary

Paired-like homeodomain transcription factor 1 (*PITX1*) was specifically up-regulated in patients with facioscapulohumeral muscular dystrophy (FSHD) by comparing the genome-wide mRNA expression profiles of 12 neuromuscular disorders. In addition, it is the only known direct transcriptional target of the double homeobox protein 4 (DUX4) of which aberrant expression has been shown to be the cause of FSHD. To test the hypothesis that up-regulation of PITX1 contributes to the skeletal muscle atrophy seen in patients with FSHD, we generated a tet-repressible muscle-specific *Pitx1* transgenic mouse model in which expression of PITX1 in skeletal muscle can be controlled by oral administration of doxycycline. After PITX1 was over-expressed in the skeletal muscle for 5 weeks, the mice exhibited significant loss of body weight and muscle mass, decreased muscle strength, and reduction of muscle fiber diameters. Among the muscles examined, the tibialis anterior, gastrocnemius, quadricep, bicep, tricep and deltoid showed significant reduction of muscle mass, while the soleus, masseter and diaphragm muscles were not affected. The most prominent pathological change was the development of atrophic muscle fibers with mild necrosis and inflammatory infiltration. The affected myofibers stained heavily with NADH-TR with the strongest staining in angular-shaped atrophic fibers. Some of the atrophic fibers were also positive for embryonic myosin heavy chain using immunohistochemistry. Immunoblotting showed that the p53 was up-regulated in the muscles over-expressing PITX1. The results suggest that the up-regulation of PITX1 followed by activation of p53-dependent pathways may play a major role in the muscle atrophy developed in the mouse model.

Key words: D4Z4, Grip strength, Rotarod, Tet-off, Cell death

Introduction

Facioscapulohumeral muscular dystrophy (FSHD) is an autosomal dominant myopathy. Patients with FSHD generally show weakness of facial and shoulder girdle muscles prior to lower limb muscles although early involvement of the lower limb muscles were reported in rare cases (Tyler and Stephens, 1950; Lunt and Harper, 1991; Padberg et al., 1991; Kilmer et al., 1995). Distinct asymmetry is a common feature of FSHD and the asymmetry can be present in the muscles of the face, shoulder girdle, and extremities (Lunt and Harper, 1991; Padberg et al., 1991; Tawil et al., 1998). Of the many forms of muscular dystrophy that exist, these particular clinical features are relatively unique to the FSHD. Many patients have additional symptoms such as severe inflammation of muscles, subclinical hearing loss, and peripheral retinal capillary abnormalities (Taylor et al., 1982; Voit et al., 1986; Arahata et al., 1995; Padberg et al., 1995b; Padberg et al., 1995a).

Genetic studies of FSHD have shown that the disease is associated with a deletion of *D4Z4* repeats in the 4q35 subtelomeric region. In non-FSHD individuals, this region contains from 11 to 100 *D4Z4* units while patients with FSHD only have one to ten *D4Z4* repeats (van Deutekom et al., 1993). Several molecular models have been proposed to explain how this deletion results in the FSHD pathology (Gabellini et al., 2002; Jiang et al., 2003; van Overveld et al., 2003; Masny et al., 2004; Wegel and Shaw, 2005; Dixit et al., 2007; Zeng et al., 2009). Most of these models suggest that the loss of *D4Z4* repeats leads to the epigenetic de-repression of one or more genes in or near the *D4Z4* array. Indeed, the deletion of *D4Z4* repeats in patients with FSHD were shown to cause the remaining *D4Z4* sequences to be hypomethylated (van Overveld et al., 2003). This hypomethylation of the *D4Z4* array was also observed in a very small population of patients with FSHD, who did not have the *D4Z4* deletion (van Overveld et al., 2003). This finding suggested that activation of a gene or genes in the *D4Z4* region causes FSHD. Several potential candidate genes have been proposed, including double homeobox protein 4 (DUX4), FSHD region gene 1 (FRG1), FSHD region gene 2 (FRG2), and adenine nucleotide translocase 1 (ANT1) (Gabellini et al., 2006; Dixit et al., 2007). A recent study conducted by Lemmers et al. suggested

that aberrant expression of DUX4 is the cause of FSHD and ruled out the possible involvement of the other candidate genes (Lemmers et al., 2010).

Each *D4Z4* repeat contains an ORF for *DUX4*, which was initially thought to be "junk" DNA due to the lack of introns and a polyadenylation signal (Gabriëls et al., 1999). The *DUX4* gene reemerged as a plausible candidate gene when studies showed that it was evolutionarily conserved and could produce a polyadenylated mRNA from the ORF in the last *D4Z4* repeat (Clapp et al., 2007; Dixit et al., 2007; Kowaljow et al., 2007; Lemmers et al., 2010). In addition, the DUX4 protein was shown to be up-regulated in the muscles of patients with FSHD, which can transcriptionally activate paired-like homeodomain transcription factor 1 (*PITX1*) (Dixit et al., 2007). In the same study, it was proposed that the DUX4 gene in the most distal *D4Z4* element was the only copy that could be transcribed into a polyadenylated mRNA. The polyadenylation will stabilize the transcript to produce a functional DUX4 protein which has been shown to be toxic to muscle cells (Kowaljow et al., 2007; Bosnakovski et al., 2009). This hypothesis was supported by the recent genetic study which showed that stable *DUX4* mRNA is essential to FSHD pathogenesis (Lemmers et al., 2010). Individuals carrying contracted D4Z4 allele without a functional polyadenylation signal of the DUX4 gene do not have the disease.

The *PITX1* gene is the only known direct transcriptional target of DUX4, and the up-regulation of *PITX1* was shown to be FSHD-specific when comparing the genome-wide mRNA profiles of FSHD to those of 11 other neuromuscular diseases (Dixit et al., 2007). The PITX1 is a homeobox transcription factor which was first recognized for its critical role in the development and postnatal function of the pituitary gland (Lamonerie et al., 1996; Tremblay et al., 1998). The gene was then reported playing important roles in hindlimb development, immune modulation and tumor suppression (Lanctôt et al., 1999; Logan and Tabin, 1999; Szeto et al., 1999; Civas et al., 2002; Kolfschoten et al., 2005; Liu and Lobie, 2007; Calvisi et al., 2011). During embryonic limb development, PITX1 only expresses in the hindlimb but not the forelimb, and determines the identity of the hindlimb (Lanctôt et al., 1999; Logan and Tabin, 1999; Szeto et al., 1999; Marcil et al., 2003). The fetuses of *Pitx1* knockout mice exhibit remarkable structural changes in their hindlimbs, such that they more resemble the forelimbs (Marcil et al., 2003). These altered limbs also exhibit left-right asymmetry in the degree of change. Chicken wing buds with mis-expressed PITX1 developed into limbs with some of the morphological characteristics of hindlimbs (Logan and Tabin, 1999). Interestingly, a polymorphism in the regulatory promoter region of *Pitx1* which reduces PITX1 expression is associated with asymmetric pelvic reduction in stickleback fish (Shapiro et al., 2004). Moreover, a mutation that abolishes the expression of PITX1 caused asymmetric lower-limb malformations in humans (Gurnett et al., 2008). Although PITX1 has been reported down regulated in cancer cells (Subramanian et al., 2004; Kolfschoten et al., 2005; Chen et al., 2007), no known disease is caused by up-regulation of PITX1 in human.

To date the function of PITX1 in postnatal muscles is not clear. We know that some homeobox proteins that play critical roles during embryonic development can also play a role in maintaining postnatal tissue identity (Leucht et al., 2008; Rinn et al., 2008). Based on this knowledge, we hypothesized that the over-expression of PITX1 in postnatal muscles may alter the homeostasis of their gene regulatory networks, which may play a key role in the pathogenesis of FSHD. The muscles of the forelimbs are likely to be more susceptible to the higher expression of PITX1 since they do not express PITX1 at high level by default. In this study, we focused our effort on the roles of PITX1 in postnatal skeletal muscles and generated a tet-repressible muscle-specific *Pitx1* transgenic mouse model which over-expresses the PITX1 in skeletal muscles, and is controlled by oral administration of doxycycline. Using this model, we can avoid over-expressing PITX1 during embryonic development, as well as study the cell autonomous effect of PITX1 in skeletal muscles.

Results

To generate the tet-repressible muscle-specific *Pitx1* transgenic mice (*TRE-Pitx1/mCK-tTA*), two transgenic mouse lines (*TRE-Pitx1* and *mCK-tTA*) were cross-bred. The *TRE-Pitx1* line carries a construct containing the *Pitx1* gene, driven by a tetracycline response element (*TRE*). The *mCK-tTA* line carries a construct containing the *tTA* gene, driven by a muscle specific creatine kinase promoter (*mCK*) as previously reported (Ghersa et al., 1998). This tet-repressible *Pitx1* transgenic mouse model allowed us to control the timing and location of PITX1 over-expression. The *Pitx1* transgenic mice over-express the PITX1 protein in skeletal muscle when oral doxycycline is not provided in the drinking water. The tissue specificity of the system was verified by assessing PITX1 expression in the skeletal muscles and organs of adult *Pitx1* transgenic mice that had been taken off doxycycline for five weeks at age of 8 weeks. RT-PCR results showed that *Pitx1* was being expressed in the muscles but not in the other organs examined (Fig. 1A). To quantify protein expression level of PITX1 in the muscle, we conducted immunoblotting using proteins from the triceps and quadricep of the *Pitx1* transgenic mice. The results showed that the PITX1 protein was 3.3 and 2.9 fold higher in the triceps and quadriceps than in those of the control mice, respectively (Fig. 1B,C).

The *Pitx1* transgenic mice developed muscle wasting and weakness

Oral doxycycline was discontinued to induce Pitx1 expression when the *Pitx1* transgenic (*TRE-Pitx1/mCK-tTA*) mice were 10 weeks old. The body weight was measured weekly. The *Pitx1* transgenic mice showed significant body weight loss (9%, $p<0.05$) compared to control mice after five weeks of PITX1 over-expression, primarily due to the loss of muscle mass (Fig. 2A). The musculature of the *Pitx1* transgenic mice was visibly reduced compared to control mice in most of the muscle groups observed (Fig. 2B). After being off doxycycline for nine to ten weeks, the mice were euthanized and masseter, soleus, tibialis anterior, quadricep, gastrocnemius, deltoid, tricep, and bicep muscles from both the left and right limbs, and the diaphragm muscles were individually dissected and weighed. Except the soleus, masseter and diaphragm, the rest of the muscles were significantly reduced in mass compared to the muscles from the control mice. For those muscles that lost muscle mass after PITX1 over-expression, the muscles of the left and right limbs were both affected significantly, except for the left biceps of the *Pitx1* transgenic mice, which did not show significant loss (Fig. 3).

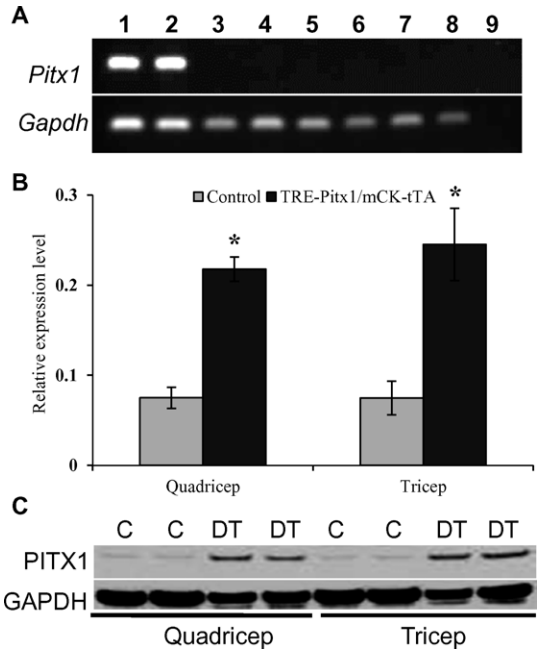

Fig. 1. Muscle-specific PITX1 over-expression in the *Pitx1* transgenic mice. (**A**) Detection of *Pitx1* mRNA expression in muscles of the *Pitx1* transgenic mice after PITX1 over-expression was induced for five weeks. *Pitx1* transcripts were detected in the two muscles, gastrocnemius and quadricep, examined (lanes 1 and 2), but not in the brain, heart, lung, liver, kidney or testis (lanes 3–8). Lane 9 is a negative control using RNA of quadricep without reverse transcriptase. (**B**) The expression levels of PITX1 protein in the triceps and quadriceps of the *Pitx1* transgenic mice and control mice (*mCK-tTA*) after PITX1 over-expression was induced for five weeks. "*" indicates $p<0.05$. (**C**) Immunoblotting images of PITX1 and GAPDH. DT, *Pitx1* transgenic mice; C, control mice. B and C showed PITX1 protein was 3.3 and 2.9 fold higher in the triceps and quadriceps than in those of the control mice, respectively.

To determine whether muscle strength and coordination were affected by PITX1 over-expression, we performed grip strength and rotarod tests to evaluate muscle function. In comparison to single transgenic control littermates the *Pitx1* transgenic mice showed no difference in grip strength or rotarod tests while still receiving oral doxycycline to suppress the *Pitx1* transgene expression. The oral doxycycline was then stopped to induce the *Pitx1* transgene expression, and the mice were tested again after three weeks. The *Pitx1* transgenic mice exhibited significant muscle weakness measured by grip strength (Fig. 4A). Although the *Pitx1* transgenic mice tended to fall off the rotarod cylinders sooner than the control mice (Fig. 4B), the difference between the groups was not statistically significant.

PITX1 over-expression leads to myofiber atrophy and muscular dystrophy

To examine the pathological changes caused by PITX1 over-expression, we performed hemotoxylin and eosin (H&E) staining to visualize the pathological changes in the myofibers. The most prominent pathological change was the angular-shaped atrophic muscle fibers in the muscle, which were not seen in the control mice. We also observed a small numbers of necrotic and centrally nucleated fibers with inflammatory infiltration, which indicates a mild degeneration/regeneration process likely in response to the muscle loss due to myofiber atrophy. Angular-shaped atrophic myofibers that strongly stained with NADH-TR have been reported in patients with FSHD (Fenichel et al., 1967; Hudgson et al., 1972; Voit et al., 1986; Kissel, 1999), therefore we performed the NADH-TR staining to determine whether similar staining patterns could be seen in the mouse model. NADH-TR staining showed that the myofibers of the *Pitx1* transgenic mice were heavily stained in general, while the angular-shaped atrophic fibers stained the darkest (Fig. 5). The myofibers with central

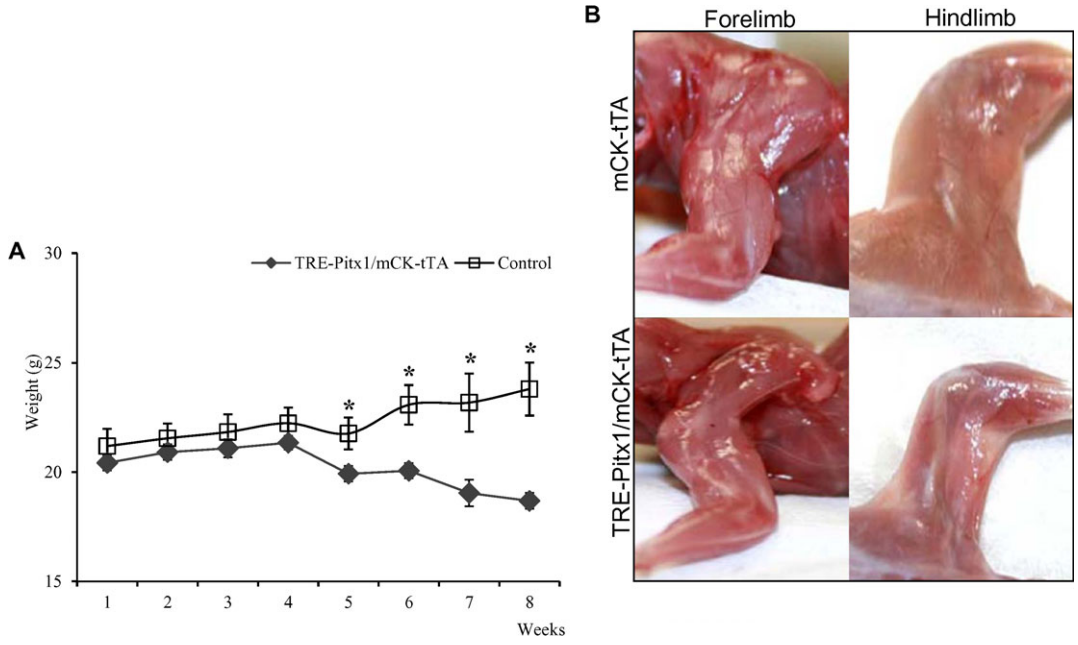

Fig. 2. The Pitx1 transgenic mice developed muscle wasting after PITX1 over-expression was induced for 5 weeks. (**A**) The average body weight (g, mean ± s.e.) of the *Pitx1* transgenic was significantly reduced compared to the control mice. The asterisks indicate significant differences with $p<0.05$. (**B**) Skeletal muscles wasting in the *Pitx1* transgenic (*TRE-Pitx1/mCK-tTA*) can be seen in both forelimb and hindlimb muscles.

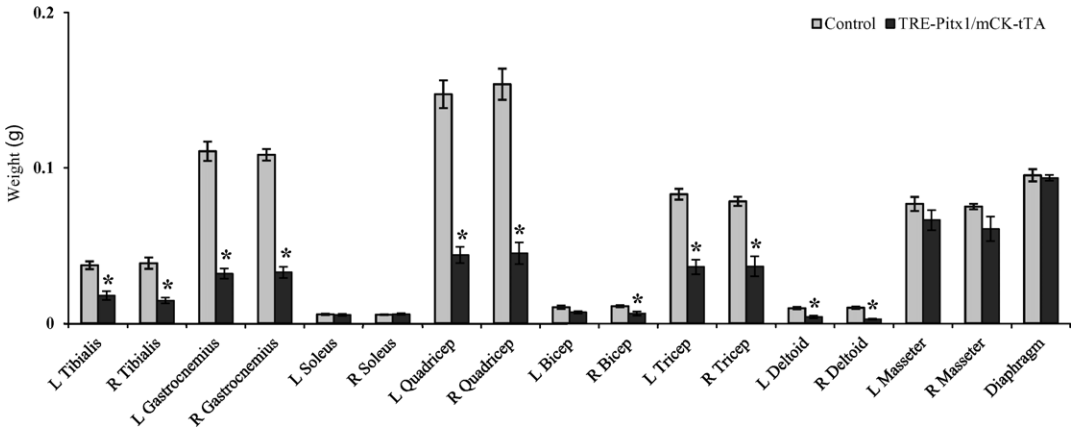

Fig. 3. The average weight (g, mean ± s.e.) of individual muscles of *Pitx1* transgenic and control mice after PITX1 over-expression for 9 weeks. The asterisks indicate significant differences with $p<0.05$.

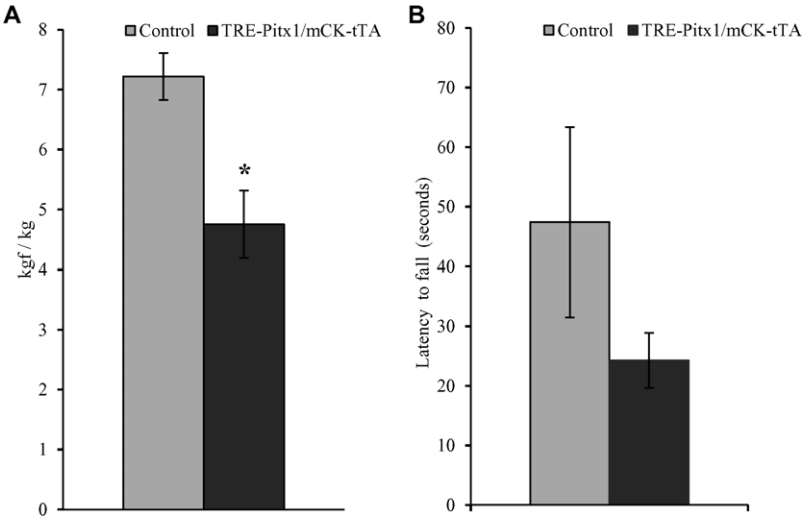

Fig. 4. Loss of muscle strength in *TRE-Pitx1/mCK-tTA* mice. Muscle functional tests showed reduced grip strength (**A**) 3 weeks after PITX1 over-expression was induced. While the *Pitx1* transgenic mice tend to fall more often, the rota rod (**B**) test did not show significant difference between the *Pitx1* transgenic mice and the control mice. The asterisks indicate significant differences with $p<0.05$.

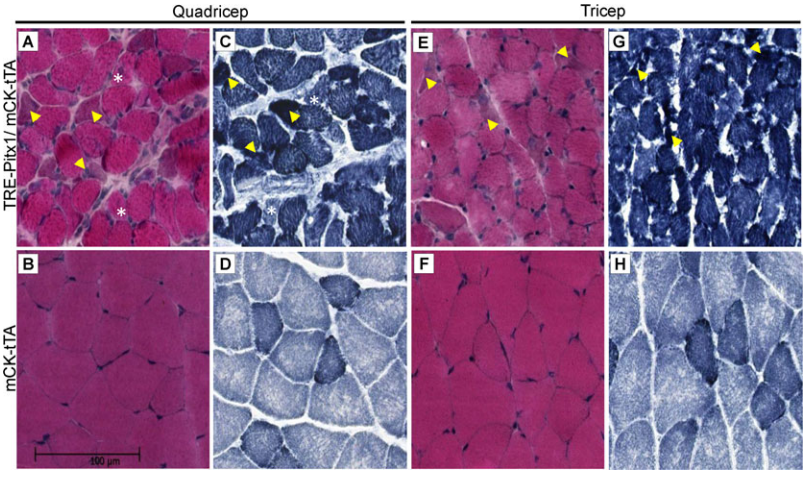

Fig. 5. NADH-TR positive angular-shaped myofibers was the most prominent pathological change observed in muscles of the *Pitx1* transgenic mice (*TRE-Pitx1/mCK-tTA*). H&E staining showed angular-shaped myofibers in both quadriceps and triceps, respectively (**A**,**E**). (**B**,**F**) H&E staining of control samples. Few of the fibers contained central nuclei suggesting the fibers were undergoing regeneration (A). NADH-TR staining showed the angular-shaped atrophic fibers were heavily stained (**C**,**G**) while the fibers with central nuclei stain lightly (C). (**D**,**H**) NADH-TR staining of control samples. Arrows indicate angular atrophic myofibers and asterisks indicate myofibers with central nuclei. Scale bar: 100 µm.

nuclei were not stained heavily with NADH-TR. Embryonic myosin heavy chain is usually expressed in small regenerating myofibers during muscle regeneration (Matecki et al., 2004). To determine whether the central nucleated myofibers were regenerating myofibers, we performed immunohistochemistry to detect embryonic myosin heavy chain in the muscles. The embryonic myosin heavy chain was detected in the cytoplasm of many myofibers which appeared to be atrophic instead of regenerating (Fig. 6). The serial sections in Fig. 6 showed the nuclei of most of the myofibers positive with embryonic myosin heavy chain located peripheral (myonuclei were visualized by PITX1 staining). The nuclei of few myofibers (lower arrow in B) slightly shifted away from the peripheral although they were not centrally localized. While some centrally nucleated fibers were positive of embryonic myosin heavy chain, others were not positive of it, suggesting not all centrally nucleated fibers are regenerating myofibers.

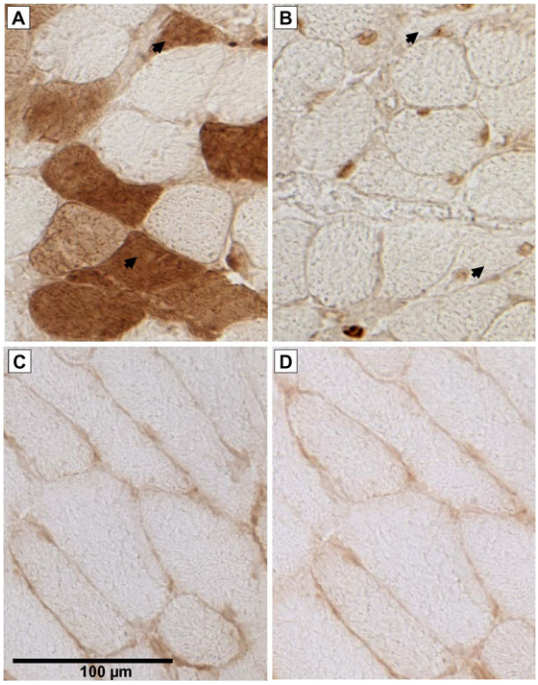

Fig. 6. Embryonic myosin heavy chain was expressed in non-regenerating myofibers of the *Pitx1* transgenic mice (*TRE-Pitx1/mCK-tTA*). (**A**) Cytoplasmic staining of the embryonic myosin heavy chain (brown) of quadriceps of the *Pitx1* transgenic mice. (**B**) Nuclear staining of PITX1 (brown) in quadriceps of the *Pitx1* transgenic mice. No staining of embryonic myosin heavy chain (**C**) and PITX1 (**D**) was seen in control mice. Arrows indicate angular atrophic myofibers. Scale bar: 100 μm.

To quantify the myofiber atrophy observed in the muscles of the *Pitx1* transgenic mice, we measured muscle fiber diameter using minimal Feret's diameter measurement, performed on cross sections stained for laminin (Briguet et al., 2004). We then ranked the myofibers based on their size, and plotted size against rank for each myofibers in order to assess the fiber size distribution using Kolmogorov-Smirnov test. There were significant differences in fiber size distribution between the *Pitx1* transgenic and control mice (Fig. 7A,B). The average fiber diameter size in the *Pitx1* transgenic mice was reduced by 45% ($p<0.05$) in the triceps and by 41% ($p<0.05$) in the quadriceps (Fig. 7C).

PITX1 provides a potential link between the DUX4 and p53 activation

The p53 tumor suppressor is a potent inducer of apoptotic cell death and p53-dependent autophagy, which was reported to be involved in modulating skeletal muscle growth (Soddu et al., 1996; Tamir and Bengal, 1998; Porrello et al., 2000). Recent studies suggested that it plays a critical role in the DUX4 induced myopathy (Wallace et al., 2011; Vanderplanck et al., 2011). To

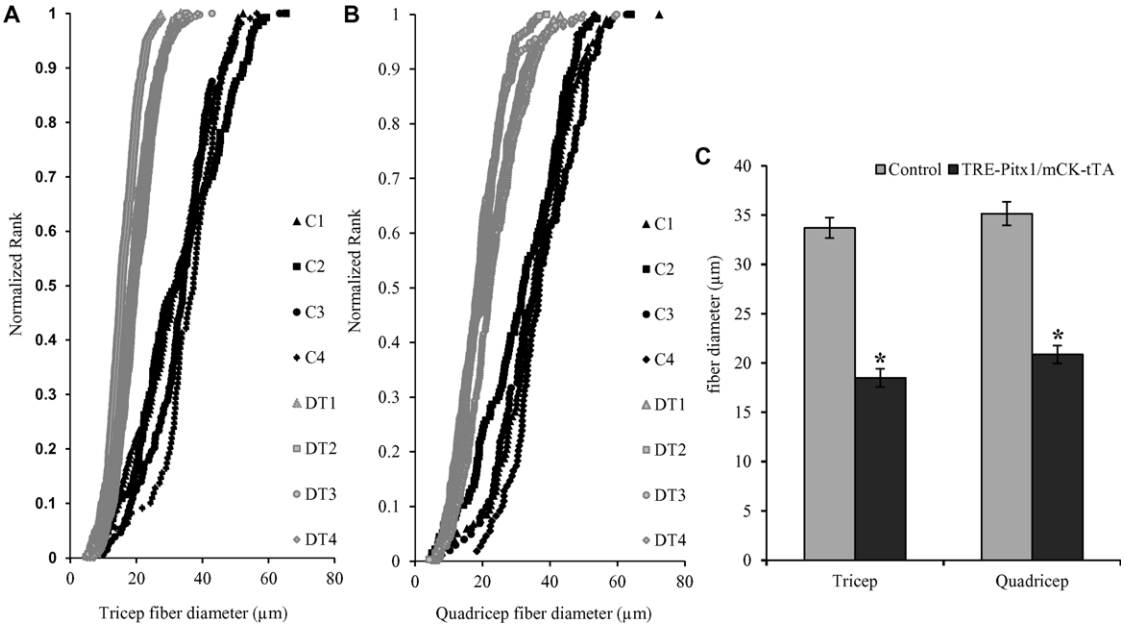

Fig. 7. Minimal Feret's diameter measurement showed the myofibers of the *Pitx1* transgenic mice (*TRE-Pitx1/mCK-tTA*) is significantly smaller compared to the control samples. The normalized rank was plotted against myofiber diameters of triceps (**A**) and quadriceps (**B**). Muscles of the *Pitx1* transgenic mice (DT1–DT4) were plotted in gray while those of control mice (C1–C4) were plotted in black. (**C**) A graphic presentation of the means of myofiber diameter. "*": $p<0.05$.

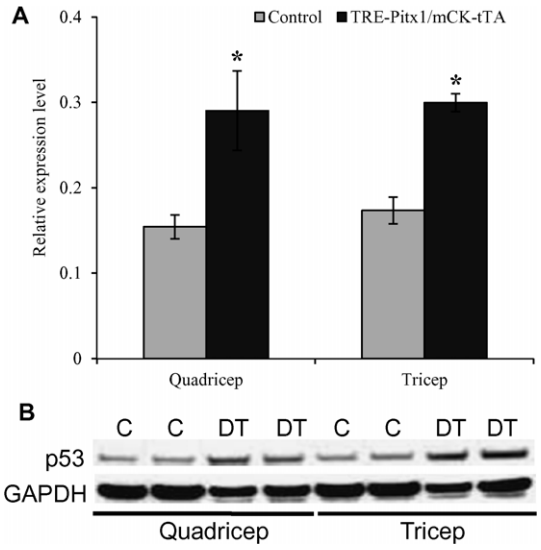

Fig. 8. p53 up-regulation in *TRE-Pitx1/mCK-tTA* mice. The tumor suppressor protein p53 was up-regulated in the *Pitx1* transgenic mice after over-expressing PITX1 for 5 weeks (**A**). "*": $p<0.05$. Immunoblotting images of p53 and GAPDH (**B**). DT, *Pitx1* transgenic mice; C, control.

determine the expression level of p53 in muscles of the *Pitx1* transgenic mice, we performed immunoblotting and found that p53 was 1.7 ($p<0.05$), and 1.9 ($p<0.05$) fold up-regulated in the triceps and quadriceps of the *Pitx1* transgenic mice, respectively (Fig. 8).

We previously reported that PITX1 was specifically up-regulated in patients with FSHD. In addition, DUX4 interacts with the *PITX1* promoter and activates the *PITX*1 expression by luciferase and electrophoretic mobility shift assays (Dixit et al., 2007). In this study, we further showed that DUX4 directly binds to the *PITX1* promoter using the ChIP assay (Fig. 9A). Quantitative PCR data showed that *PITX1* promoter was enriched 8.4-fold in comparison to negative control. The enrichment was not seen in the GFP transfected samples (Fig. 9B). The data generated in the study provided evidence of a regulatory cascade from DUX4 to PITX1 followed by p53 induction.

Discussion

Due to the lack of an ortholog of DUX4 in the mouse genome, the attempt to generate and study a *Dux4* transgenic mouse model has been challenging (Bosnakovski et al., 2009). Therefore, generating animal models to study genes or pathways directly regulated by DUX4 becomes a valuable alternative approach for understanding the disease mechanisms. In this study, our results showed that the *Pitx1* transgenic mice developed phenotypes similar to those of patients with FSHD, including the wasting of selective groups of muscles and the NADH-TR positive atrophic myofibers often seen in FSHD biopsies (Fenichel et al., 1967; Hudgson et al., 1972; Slipetz et al., 1991; Kissel, 1999). We further showed that the p53 pathway, which was recently reported to be involved in DUX4 induced myopathy *in vivo,* was up-regulated by PITX1 over-expression. The findings in this study provide links between aberrant DUX4 expression, up-regulation of PITX1, the activation of the p53-dependent cell death pathways, and the down-stream muscular dystrophy phenotype.

In addition to the myofiber atrophy that occurs in some inherited muscle diseases (Emery, 2002), skeletal muscle atrophy occurs when the muscle is disused, immobilized, denerved and during starvation (Andersen et al., 1999; Jagoe et al., 2002; Jackman and Kandarian, 2004). Muscle atrophy also occurs under other disease conditions such as cancer cachexia, kidney disease, and mitochondrial diseases (Tisdale, 1997; Qureshi et al., 1998; Weissman et al., 2008). Many molecular pathways have been reported to be involved in the muscle atrophy process (Bodine et al., 2001b; Bodine et al., 2001a; Pallafacchina et al., 2002; Mammucari et al., 2007). Among the known pathways, several studies showed that p53 plays critical roles in myogenesis and muscle wasting (Soddu et al., 1996; Tamir and Bengal, 1998; Porrello et al., 2000). The p53 protein was shown to be activated during myoblast differentiation. Through a protein-protein interaction with MyoD, it transcriptionally activates muscle creatin kinase (MCK), a late muscle differentiation marker (Tamir and Bengal, 1998). Several studies showed that p53 is required for TNF-mediated inhibition of muscle differentiation as well as the tumor-load mediated muscle atrophy (Coletti et al., 2002; Schwarzkopf et al., 2006; Moresi et al., 2008). A mouse model with a stable and chronically activated p53 protein develops muscle atrophy at 18–24 months of age, although the mice are more resistant to cancer (Tyner et al., 2002). In healthy tissues and cells, the p53 protein level is low with cytoplasmic localization. Upon activation in response to stress signals (such as DNA damage, UV radiation and hypoxia) p53 translocates to the cell nuclei and activates downstream genes and pathways involved in cell survival and apoptosis (Aranda-Anzaldo et al., 1999; Vousden, 2000). It has been shown that over-expression of DUX4 in murine C2C12 and human rhabdomyosarcoma cells

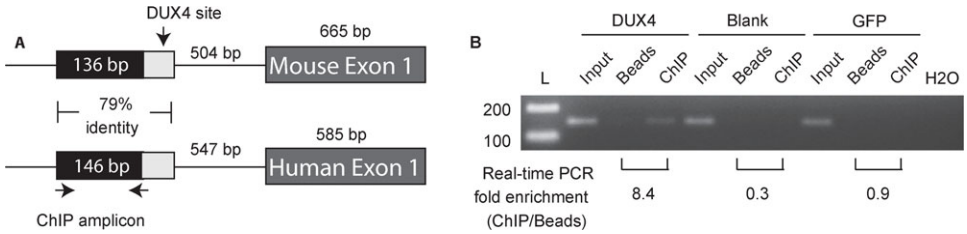

Fig. 9. Chromatin immunoprecipitation demonstrates DUX4 binding of the *PITX1* promoter. (**A**) Diagram of the mouse and human *PITX1* promoters, which share high identity for non-coding DNA regions. The grey box indicates the position of the conserved DUX4 binding site, which sits immediately adjacent to the *PITX1* promoter ChIP amplicon (black box). (**B**) Representative PCR amplification of the *PITX1* promoter following DUX4 ChIP (from 3 independent experiments). The amplicon of *PITX1* promoter was enriched 8.4-fold following DUX4 ChIP whereas negative control blank and GFP showed no enrichment in comparison to the beads control. L, 100 bp ladder.

induce cell death through apoptosis (Kowaljow et al., 2007). The toxic effect of DUX4 over-expression was recently confirmed *in vivo*. In that study, the p53-dependent cell death pathway was identified to be the cause of the DUX4 induced myopathy, although the mechanistic link between DUX4 and p53 was not clear (Wallace et al., 2011). In this study, we showed that over-expression of PITX1 up-regulated p53 expression, which provides a potential link between DUX4 and p53 activation in muscles.

Down-regulation of PITX1 expression has been observed in several cancers including lung, colon, prostate and bladder cancers (Singh et al., 2002; Subramanian et al., 2004; Kolfschoten et al., 2005; Chen et al., 2007). In addition to its role in muscle development, recent studies showed that PITX1 also acts as a tumor suppressor. Up-regulation of PITX1 induces apoptosis in cancer cells through the activation of the p53-dependent cell death pathway (Liu and Lobie, 2007; Yamaguchi et al., 2010; Calvisi et al., 2011). In addition, PITX1 suppresses telomerase reverse transcriptase (TERT) transcription through direct binding to the TERT promoter, which reduces the telomerase activity that maintains telomere length in cancer cells (Qi et al., 2011). In the p53-dependent pathway, PITX1 was shown to bind directly to the regulatory elements of the p53 promoter, and activates p53 transcription with subsequent apoptosis in human mammary carcinoma cells (Liu and Lobie, 2007). Recently, p53 and its regulatory targets were reported to be up-regulated in FSHD (Tsumagari et al., 2011; Vanderplanck et al., 2011). In addition, treatment with antisense oligonucleotides targeting *DUX4* reduced the expression of p53 in patients' myoblasts. Although not directly examined, several studies suggested that apoptosis is likely to be involved in the pathogenesis of FSHD. For example, genes involved in apoptosis such as BCL2-associated X protein (BAX), B-cell lymphoma 2 (BCL2) and Caspase-3, Caspase-2, Caspase-6, Caspase-8, and Granzyme-B, have been reported to be up-regulated in the muscles of patients with FSHD (Sandri et al., 2001; Winokur et al., 2003; Laoudj-Chenivesse et al., 2005). Our findings support that the p53-depedent cell death pathways might be involved in FSHD pathogenesis, and needs to be further studied.

In our study, the decrease in muscle mass of the *Pitx1* transgenic mice is primarily due to muscle atrophy, which was observed soon after inducing PITX1 over-expression. Histological examination showed dystrophic features including large number of atrophic myofibers, mild cellular infiltration, and some necrotic and central nucleated fibers. Myofiber necrosis, regeneration, inflammatory infiltration, and fibrosis are common pathologies seen in several muscular dystrophies, including FSHD (Taylor et al., 1982; Lin and Nonaka, 1991; Arahata et al., 1995; Neudecker et al., 2004; Reilich et al., 2010). In addition to these pathological changes, muscle atrophy with marked numbers of angular-shaped atrophic fibers was also observed in FSHD muscle (Fenichel et al., 1967; Furukawa et al., 1969; Voit et al., 1986; Lin and Nonaka, 1991; Arahata et al., 1995; Kissel, 1999). While myofiber atrophy due to denervation/renervation generally involves "grouped" angular-shape atrophic fibers, atrophic myofibers with a myogenic cause tend to be scattered (Banker, 1986; Benedetti et al., 2005). The angular myofibers in FSHD were proposed to be due to a myogenic cause due to their scattered distribution (Engel and Kossman, 1963; Lin and Nonaka, 1991; Nakagawa et al., 1997). We observed the same scattered distribution of angular-shaped myofibers in the *Pitx1* transgenic mice muscles. In addition, angular-shaped atrophic fibers that strongly stain with NADH-TR and myofibers that are positive for embryonic myosin heavy chain are found in both patients with FSHD and our *Pitx1* transgenic mice (Fenichel et al., 1967; Hudgson et al., 1972; Voit et al., 1986; Kissel, 1999).

Regenerating myofibers that are positive for embryonic myosin heavy chain are seen in muscular dystrophies and mouse models of those diseases (Chen et al., 2000; Matecki et al., 2004). These regenerating fibers are usually small in size, clustered in groups and centrally nucleated. Here we show that the myofibers undergoing muscle atrophy can also express embryonic myosin heavy chain. Most of the fibers positive for embryonic myosin heavy chain in the *Pitx1* transgenic mice do not show characteristics of regenerating myofibers. Instead they show feature of atrophic fibers. We hypothesize that the expression of the embryonic myosin heavy chain in the affected fibers is part of a compensatory response to the ongoing muscle atrophy process.

During embryonic development, the expression of PITX1 was observed high in hindlimb but not in the forelimb, which plays a critical role to hindlimb identify (Lanctôt et al., 1999; Logan and Tabin, 1999; Szeto et al., 1999). Interestingly PITX1 has been shown to have a left-right asymmetric effect when the expression level of the gene was reduced or eliminated (Lanctôt et al., 1999; Marcil et al., 2003; Shapiro et al., 2004). Since the facial and certain muscles in the shoulder girdle are the most affected in patients with FSHD, and the weakness can often be asymmetric, it would be important to determine whether a similar pattern of muscle involvement can be seen in our mouse model. It is known that specific groups of muscles (ex. facila, pectoralis major, zygomaticus, orbicularis oris, triceps, biceps and trapezius muscles) of patients with FSHD are affected earlier, while some are affected later (tibialis, foot extensor, gastrocnemius, quadricep and abdominal muscles) (Tyler and Stephens, 1950; Lunt and Harper, 1991; Olsen et al., 2006; Castellano et al., 2008; Reilich et al., 2010) or generally spared (ex. deltoid, bulbar, masseter, gluteal, peroneal extraocular, pharyngeal, lingual and cardiac muscles) (Padberg et al., 1991; Tawil et al., 1998; Olsen et al., 2006; Tawil and Van Der Maarel, 2006; Reilich et al., 2010). In addition, the muscle weakness can often to be left-right asymmetric (Brouwer et al., 1991; Lunt and Harper, 1991; Tawil et al., 1998). To determine whether selected muscle groups of the *Pitx1* transgenic mice are affected differentially, and whether the muscle atrophy is left-right asymmetric, we collected and weighed both the left and right tibialis, gastrocnemius, soleus, quadricep, bicep, tricep, deltoid and masseter muscles of the *Pitx1* transgenic and control mice. Indeed, the masseter and diaphragm muscles, which are usually spared in patients with FSHD, were also not affected in the *Pitx1* transgenic mice. Most of the limb muscles except the soleus developed muscle atrophy and lost significant muscle weight. No left-right asymmetric involvement was observed in most of the muscles examined. Only the biceps of the *Pitx1* transgenic mice showed asymmetry. The biceps is one of the muscles that is most affected in patients with FSHD, and can be asymmetrically affected. Detailed pathological examination of the muscles collected from both sides will provide additional information for evaluating the asymmetric involvement of the biceps.

Transcription factor PITX2 is in the same protein family as PITX1. During early embryogenesis, PITX2 is a key regulator in establishing embryo left-right asymmetry (Yoshioka et al., 1998).

PITX2-deficient mice are embryonic lethal and show severe defects in heart, eye, pituitary gland and tooth organogenesis (Kioussi et al., 2002). PITX2 was shown expressed in limb muscle precursors during embryonic development and can transcriptionally activate *MyoD* in the cells (L'Honoré et al., 2007; Shih et al., 2007; L'Honoré et al., 2010; Zacharias et al., 2011). PITX1 and PITX2 have been shown to be either co-regulated or functionally overlapped in multiple organs including hindlimb during embryonic development (St Amand et al., 2000; Marcil et al., 2003; Lamba et al., 2008; Castinetti et al., 2011). Considering the critical role of PITX2 in left-right asymmetry and limb development, it is possible that PITX2 is involved in the pathology seen in this model. Based on unpublished microarray data generated in our lab, we did not see expression change of the *Pitx2* transcript in the *Pitx1* transgenic mice, suggesting PITX2 is not involved in the myopathy caused by over-expressing PITX1.

In this study, we characterized a mouse model that conditionally over-expresses PITX1 in skeletal muscles, and showed that the mice exhibit phenotypes of muscle weakness and myopathy. In addition, our data suggest a regulatory cascade from DUX4, PITX1 to p53.

Materials and Methods

Generation of the tet-repressible muscle-specific transgenic *Pitx1* mouse

All animal procedures were approved by the IACUC committee at the Children's National Medical Center in Washington, DC. Two transgenic mouse lines (*TRE-Pitx1* and *mCK-tTA*) were cross-bred in order to generate the tet-repressible muscle-specific *Pitx1* transgenic mice (*TRE-Pitx1/mCK-tTA*). The *TRE-Pitx1* line carries a construct containing the *Pitx1* gene, driven by a tretracycline response element (*TRE*). The *mCK-tTA* line carries a construct containing the *tTA* gene, driven by a muscle specific creatine kinase promoter (*mCK*) as previously reported (Ghersa et al., 1998). To generate the *TRE-Pitx1* mice, the *Pitx1* coding sequence from MGC-13954 (ATCC) was subcloned into the pBI-G vector (Clontech, Mountain View, CA, USA) by *Not1* and *Sal1* digestion (Invitrogen, Carlsbad, CA, USA), followed by restriction site blunting with klenow DNA Polymerase I (Invitrogen, Carlsbad, CA, USA). The pBI-G vector was prepared by *Not1* digestion, followed by restriction site blunting with klenow DNA Polymerase I. After being purified by Qiagen purification kit (Qiagen, Germantown, MD, USA), the blunt ends were dephosphorylated with calf intestine phosphatase (CIP) (New England Biolabs, Ipswich, MA, USA) at 37℃ for one hour. The *Pitx1* and vector fragments were ligated together via T4 DNA ligase overnight incubation at 16℃. The insertion of the *Pitx1* fragment into the vector was validated by nucleotide sequencing (Beckman Coulter, Danvers, MA, USA). The backbone of the *pBI-G-Pitx1* vector was removed via *AclI* and *AseI* (New England Biolabs, Ipswich, MA, USA) digestion, followed by gel purification with a GELase Agrose gel-digestion preparation kit (Epicentre Biotechnologies, Madison, WI, USA). The purified construct was microinjected (10 ng/μl) into the pronuclei of B6CBAF1 fertilized 0.5 day old mouse oocytes. The injected oocytes were then transferred to the oviducts of pseudopregnant ND4 outbred foster mothers.

The founder female mouse with the *TRE-Pitx1* transgene was bred with a C57Bl/10 male to expand the line. The *Pitx1* transgenic mice were generated by cross-breeding the *TRE-Pitx1* and *mCK-tTA* mice. The female mice received drinking water with doxycycline (200 ug/ml with 5.0% sucrose) in order to suppress the *Pitx1* transgene expression in the pups *in utero*. Under these conditions, the *TRE-Pitx1/mCK-tTA Pitx1* transgenic mice were born at the expected Mendelian ratio. The pups continued to receive doxycycline through the mother's milk. After weaning, all pups were maintained on water treated with doxycycline until they were entered into an experimental regime. For all experiments, littermates carrying a single transgene (*Pitx1* or *tTA*) were used as controls.

To identify mice carrying one or two of the transgenes (*Pitx1* and *tTA*), we collected a small piece of tail tip and isolated DNA for genotyping. The following primers were used for polymerase chain reaction (PCR) amplification. For *Pitx1*: forward 5′-TGG AGG CCA CGTTCC AAA G-3′ and reverse 5′- GTTCTTGAA-CCAGACCCGCAC-3′; for *tTA*: forward 5′-ACAGCGCATTAGAGCTGCTT-3′ and reverse 5′-CCCCTTCTAAAGGGCAAAAG -3′.

Body and muscle mass

We removed doxycycline from the water of 9 *Pitx1* transgenic (*TRE-Pitx1/mCK-tTA*) mice and the control littermate mice (*TRE-Pitx1* or *mCK-tTA*) at 10 weeks old, and measured their body weight weekly, starting from the date that doxycycline was first removed from their water. After being off doxycycline for nine to ten weeks, the mice were euthanized. Masseter, soleus, tibialis anterior, quadriceps, gastrocnemius, deltoid, triceps, biceps and the diaphragm from five *Pitx1* transgenicand control mice were dissected and immediately weighed. The data were expressed as the mean ± s.e. Significant differences between the induced *Pitx1* transgenic mice and the controls were tested by 2-tailed T test. The significance cutoff was $p<0.05$.

Reverse transcription-polymerase chain reaction (RT-PCR)

Total RNA was extracted from tissues using the Trizol reagent (Invitrogen, Carlsbad, CA, USA), following the manufacturer protocol. Briefly, 1 μg total RNA was first treated with DNaseI, followed by single strand cDNA synthesis using oligo dT and Superscript II RT (Invitrogen, Carlsbad, CA, USA). Primers used for amplifying *Pitx1* transcripts are as follows: forward 5′-TGG AGG CCA CGT TCC AAA G-3′ and reverse 5′- GTT CTT GAA CCA GAC CCG CAC-3′. The PCR condition was 35 cycles of 94℃ for 45 second, 57.5℃ for 45 second, followed by 72℃ for 1 minute 30 second. The amplified product was visualized on a 2% agarose gel (Gibco BRL, Gaithersburg, MD, USA).

Immunoblotting

Muscle sections were digested with a hand sonicator for 10 seconds at room temperature in lysis buffer (50 mM Tris-HCL, pH 7.5, 150 mM NaCl, 0.5% sodium deoxycholate, 1% NP40, 0.1% SDS, and protease inhibitor). Protein concentration was determined by DC protein assay (Bio-Rad, Hercules, CA, USA), and 30 μg of protein was loaded to 4–12% Bis-Tris NuPage Mini Gels (Invitrogen, Carlsbad, CA, USA) then transferred to Hybond nitrocellulose membranes (Amersham Biosciences, Little Chalfont, Buckinghamshire, UK). After blocking, the membrane was incubated with rabbit polyclonal anti-PITX1 antibody (1:2,000) (Dixit et al., 2007), anti-p53 (1:500) (Santa Cruz Biotechnology, Santa Cruz, CA, USA) followed by secondary antibodies conjugated with HRP (Amersham Biosciences, Little Chalfont, Buckinghamshire, UK). Chemiluminescent substrate (Pierce, Rockford, IL, USA) was used to visualize the target proteins on blue light autorad film (BioExpress, Kaysville, UT, USA). Detection of loading control GAPDH (Santa Cruz Biotechnology, Santa Cruz, CA, USA) was similarly performed with 1:1000 dilution of the mouse monoclonal primary antibody. Band density of the target protein was measured using a GS 800 Calibrated Densitometer (Bio-Rad, Hercules, CA, USA) then normalized to the density of GAPDH.

Muscle function testing

The grip strength test (Grip Strength Meter, Columbus Instruments, Columbus, OH, USA) and the rotarod test (Columbus Instruments, Columbus, OH, USA) were performed on 7 *Pitx1* transgenic mice and 7 control littermates. The mice were 14 weeks old when the doxycycline was removed from their drinking water. The functional tests were performed twice: before the mice were off doxycycline and 3 weeks after the mice were off doxycycline.

The Grip Strength Meter (GSM) consists of two steel grids connected to force meters. The forelimb grid is horizontal and the hind limb grid is angled. Grip strength is tested by holding the mouse over the grid until the mouse can grip the steel bars. Then the mouse is pulled away from the force meter until it releases the grid. The meter records the maximum force that was applied. The mice were acclimated to the GSM for five minutes, one day prior to data collection. They were then tested once a day for five consecutive days; five measurements were recorded for each test. The largest measurements from each of the five tests were averaged and normalized to body weight (kg).

For the rotarod test, the mice were acclimated to the rotarod apparatus for two consecutive days prior to data collection. During acclimation the mice were placed on the rotarod twice a day for two minutes, at a speed of 5 rotations per minute. If the mice fell off the cylinder before the two minutes were up, they were placed back on the cylinder. The mice were then tested twice a day for three consecutive days. During each test, the cylinder was set at a speed of 10 rotations per minute for one minute. If the mice fell off the cylinder before the minute was up, they were placed back on the cylinder. After one minute the speed accelerated at a rate of 1.2 rotations per second until it reached 40 rotations per minute. Starting at the beginning of the acceleration phase, the length of time (in seconds) that each mouse could stay on the cylinder before falling off was recorded. The maximal running time is 180 seconds. The final score was determined by averaging the recorded time from all six trials.

Histology, NADH-TR staining, immunohistochemistry, and fiber diameter

Eight week-old mice were off oral doxycycline for 5 weeks before muscle collection. Immediately after dissection, the whole muscles were snap-frozen in isopentane cooled with liquid nitrogen, then stored at −80℃ until sectioning. A Leica CM 1900 cryostat (Walldorf, Baden-Wurttenberg, Germany) was used to prepare cryosections for all the following histological analyses. H&E staining was conducted using 8 μm sections. Five random non-overlapping fields of the tissue section were imaged using Nikon Eclipse E800 microscope (Nikon, Chiyoda-ku,

Tokyo, Japan), RT slider camera (Diagnostic Instrument, Sterling Height, MI, USA) and SPOT advanced software.

For NADH-TR staining, 12 μm cryosections were prepared then incubated in solution with NBT (Nitro-blue tetrazolium 200 mg, Tris buffer 100ml) (Sigma, Saint Louis, MO, USA) and NADH (NADH 20mg, Tris buffer 50 ml) (Sigma, Saint Louis, MO, USA) at 37℃ for 30 minutes. The sections were then washed three times with deionzed H_2O, followed by serial acetone immersions at the following concentrations: 30%, 60%, 90%, 60%, and 30%. The sections were washed three times with deionzed H_2O before being mounted with aqueous medium.

For immunohistochemistry, 4 μm muscle sections were fixed in cold acetone for 10 min, and then incubated with primary antibody at 4℃ overnight. The primary antibodies used for PITX1 and embryonic myosin heavy chain detection is rabbit polyclonal anti-PITX1 (1:500) (Dixit et al., 2007) and mouse monoclonal anti-embryonic myosin heavy chain antibody F1.652 (Hybridoma bank, Iowa City, Iowa, USA) (1:20), respectively. The ABC kit (Vectors Lab, Burlingame, CA, USA) was then used to detect the primary antibody bound target proteins. The sections were stained with nuclear dye Hoechst 33258 (1:2500 dilution) to visualize nuclei. The muscle sections were imaged using Nikon Eclipse E800 microscope, RT slider camera and SPOT advanced software. To measure myofiber diameter, 6 μm cryosections were prepared from the muscles of 4 *Pitx1* transgenic and 4 control littermates. The sections were fixed using cold acetone, blocked using 10% horse serum, and then incubated with rabbit anti-laminin antibody (Sigma, Saint Louis, MO, USA) at a dilution of 1:400. After the sections were washed three times with PBS, we applied Cy2 donkey anti-rabbit antibody (Jackson ImmunoResearch, West Grove, PA, USA) at a dilution of 1:500. The images of 5 random fields were processed using Image J software (NIH) and the minimal Feret's diameter was measured. To obtain the actual micron size we set a scale using a microscope scale (Graticules) where 1 pixel =5.40 μm. The fibers were first ranked based on their size than the rank number was divided by the total number of fibers to obtain a value between 0 to1. This number (Y-axis) is then plotted against the fiber diameter (X-axis). The Kolmogorov-Smirnov test was used to determine the significance of the difference in fiber size distribution (http://www.physics.csbsju.edu/stats/KS-test.n.plot_form.html).

Chromatin immunoprecipitation (ChIP)

HEK293 cells were grown in DMEM supplemented with 10% FBS. Five million cells were transfected with AAV.CMV.hrGFP or AAV.CMV.DUX4.V5 proviral plasmids (Wallace et al., 2011). After 48 hrs, cells were cross-linked with 1% formaldehyde and cross linking was stopped after 10 min using 0.125 M glycine. Chromatin was extracted with ChIP lysis buffer (1% SDS; 10 mM EDTA, pH 8.0; 50 mM Tris-Cl, pH 8.0; 1 mM PMSF; 1× cocktail protease inhibitor) Chromatin was sheared on ice to 300~600 bp by sonication (Sonics, Newtown, CT, USA) and 800 μg were pre-cleared with protein G-agarose beads (Invitrogen, Carlsbad, CA, USA), followed by immunoprecipitation with 5 μg agarose conjugated-V5 antibody (Bethyl Laboratories, Montgomery, TX, USA) at 4℃ overnight. The immune complexes were washed sequentially with low salt (0.1% SDS; 2 mM EDTA, pH 8.0; 20 mM Tris-Cl, pH 8.0; 150 mM NaCl; 1% Triton X 100), high salt (0.1% SDS; 2 mM EDTA, pH 8.0; 20 mM Tris-Cl, pH 8.0; 500 mM NaCl; 1% Triton X 100), LiCl wash buffer (2 mM EDTA, pH 8.0; 20 mM Tris-Cl, pH 8.0; 250 mM LiCl; 1% NP-40; 1% deoxycholate) and TE buffer DNA-protein complexes were reverse cross-linked using 5 M NaCl. DNA was purified and resuspended in 30 μl H_2O. SYBR-green real-time PCR was performed with the following primers using 1 μl of ChIP DNA: *PITX1* 5′-CCTAAGGTGTAAAA-CAAGGGGAGAG-3′ (forward); 5′-CGGGATTGGGATAGAAATGATGG-3′ (reverse) and a 55℃ annealing temperature. These primers amplify a specific, 146 bp DNA fragment located 641 bp upstream of the *PITX1* exon 1 and 64 bp upstream of a DUX4 binding site located in the *PITX1* promoter (Dixit et al., 2007). In addition to real-time PCR, *PITX1* amplicons were also electrophoresed on 1.5% agarose gel and visualized by ethidium bromide staining. Data shown are representative of three independent experiments. Input DNA controls were diluted 1:200 prior to PCR. Real-time PCR signal was normalized to a standard curve and fold enrichment was calculated using a "signal over background method" as per manufacturer's instructions (http://www.invitrogen.com/site/us/en/home/Products-and-Services/Applications/epigenetics-noncoding-rna-research/Chromatin-Remodeling/Chromatin-Immunoprecipitation-ChIP/chip-analysis.html). Reported values represent the ratio of *PITX1* signal in ChIP samples over beads (without antibody) control samples.

Acknowledgements

We thank the FSH society for the support of generating the *Pitx1* mouse model. S.N.P. and J.C. are supported by NIH/NIAMS1R01AR052027. Y.-W.C. is partially supported by NIH/NICHD1R24HD050846 and NIH/NIAMS1R01AR052027. R.S. and M.D. were supported by NIH/NICHD1U54HD05317701A1. J.L. is supported by NIH/NINDS 1R21NS072260-01. S.Q.H is supported by NIH/NINDS 1R21NS072260-01, MDA 218892, FSH society and startup funds from the research institute at nationwide children's hospital. This work is supported by National Institute of Health [1R01AR052027 to S.N.P., J.C., Y.-W.C., 1R24HD050846 to Y.-W.C., U54HD05317701A1 to R.S., M.D., 1R21NS072260-01 to J.L., S.Q.H.]; and the Facioscapulohumeral Muscular Dystrophy Society [FSHSMGBF011 to Y.-W.C.]; and Muscular Dystrophy Association [MDA 218892 to S.Q.H.]. S.N.P. and J.C. characterized the *Pitx1* transgenic mice phenotypes and wrote up the manuscript with Y.-W.C. The studies were designed by Y.-W.C. with input from M.S., and K.N., R.S., M.D., S.M. and M.S. contributed to the generation of the *TRE-Pitx1* transgenic mice. K.N. provided the *mCK-tTA* mice and assisted data interpretation. J.L. and S.Q.H performed experiments and analyzed the ChIP assay.

Competing Interests

The authors declare that there are no competing interests.

References

Andersen, J. L., Gruschy-Knudsen, T., Sandri, C., Larsson, L. and Schiaffino, S. (1999). Bed rest increases the amount of mismatched fibers in human skeletal muscle. *J. Appl. Physiol.* **86**, 455-460.

Arahata, K., Ishihara, T., Fukunaga, H., Orimo, S., Lee, J. H., Goto, K. and Nonaka, I. (1995). Inflammatory response in facioscapulohumeral muscular dystrophy (FSHD): immunocytochemical and genetic analyses. *Muscle Nerve* **18 S13**, S56-S66.

Aranda-Anzaldo, A., Orozco-Velasco, F., García-Villa, E. and Gariglio, P. (1999). p53 is a rate-limiting factor in the repair of higher-order DNA structure. *Biochim. Biophys. Acta* **1446**, 181-192.

Banker, B. Q. (1986). Arthrogryposis multiplex congenita: spectrum of pathologic changes. *Hum. Pathol.* **17**, 656-672.

Benedetti, S., Bertini, E., Iannaccone, S., Angelini, C., Trisciani, M., Toniolo, D., Sferrazza, B., Carrera, P., Comi, G., Ferrari, M. et al. (2005). Dominant LMNA mutations can cause combined muscular dystrophy and peripheral neuropathy. *J. Neurol. Neurosurg. Psychiatry* **76**, 1019-1021.

Bodine, S. C., Stitt, T. N., Gonzalez, M., Kline, W. O., Stover, G. L., Bauerlein, R., Zlotchenko, E., Scrimgeour, A., Lawrence, J. C., Glass, D. J. et al. (2001a). Akt/mTOR pathway is a crucial regulator of skeletal muscle hypertrophy and can prevent muscle atrophy in vivo. *Nat. Cell Biol.* **3**, 1014-1019.

Bodine, S. C., Latres, E., Baumhueter, S., Lai, V. K., Nunez, L., Clarke, B. A., Poueymirou, W. T., Panaro, F. J., Na, E., Dharmarajan, K. et al. (2001b). Identification of ubiquitin ligases required for skeletal muscle atrophy. *Science* **294**, 1704-1708.

Bosnakovski, D., Daughters, R. S., Xu, Z., Slack, J. M. and Kyba, M. (2009). Biphasic myopathic phenotype of mouse DUX, an ORF within conserved FSHD-related repeats. *PLoS ONE* **4**, e7003.

Briguet, A., Courdier-Fruh, I., Foster, M., Meier, T. and Magyar, J. P. (2004). Histological parameters for the quantitative assessment of muscular dystrophy in the mdx-mouse. *Neuromuscul. Disord.* **14**, 675-682.

Brouwer, O. F., Padberg, G. W., Ruys, C. J., Brand, R., de Laat, J. A. and Grote, J. J. (1991). Hearing loss in facioscapulohumeral muscular dystrophy. *Neurology* **41**, 1878-1881.

Calvisi, D. F., Ladu, S., Conner, E. A., Seo, D., Hsieh, J. T., Factor, V. M. and Thorgeirsson, S. S. (2011). Inactivation of Ras GTPase-activating proteins promotes unrestrained activity of wild-type Ras in human liver cancer. *J. Hepatol.* **54**, 311-319.

Castellano, V., Feinberg, J. and Michaels, J. (2008). Facioscapulohumeral dystrophy: case report and discussion. *HSS J.* **4**, 175-179.

Castinetti, F., Brinkmeier, M. L., Gordon, D. F., Vella, K. R., Kerr, J. M., Mortensen, A. H., Hollenberg, A., Brue, T., Ridgway, E. C. and Camper, S. A. (2011). PITX2 AND PITX1 regulate thyrotroph function and response to hypothyroidism. *Mol. Endocrinol.* **25**, 1950-1960.

Chen, Y. W., Zhao, P., Borup, R. and Hoffman, E. P. (2000). Expression profiling in the muscular dystrophies: identification of novel aspects of molecular pathophysiology. *J. Cell Biol.* **151**, 1321-1336.

Chen, Y., Knösel, T., Ye, F., Pacyna-Gengelbach, M., Deutschmann, N. and Petersen, I. (2007). Decreased PITX1 homeobox gene expression in human lung cancer. *Lung Cancer* **55**, 287-294.

Civas, A., Island, M. L., Génin, P., Morin, P. and Navarro, S. (2002). Regulation of virus-induced interferon-A genes. *Biochimie* **84**, 643-654.

Clapp, J., Mitchell, L. M., Bolland, D. J., Fantes, J., Corcoran, A. E., Scotting, P. J., Armour, J. A. and Hewitt, J. E. (2007). Evolutionary conservation of a coding function for D4Z4, the tandem DNA repeat mutated in facioscapulohumeral muscular dystrophy. *Am. J. Hum. Genet.* **81**, 264-279.

Coletti, D., Yang, E., Marazzi, G. and Sassoon, D. (2002). TNFalpha inhibits skeletal myogenesis through a PW1-dependent pathway by recruitment of caspase pathways. *EMBO J.* **21**, 631-642.

Dixit, M., Ansseau, E., Tassin, A., Winokur, S., Shi, R., Qian, H., Sauvage, S., Mattéotti, C., van Acker, A. M., Leo, O. et al. (2007). DUX4, a candidate gene of

facioscapulohumeral muscular dystrophy, encodes a transcriptional activator of PITX1. *Proc. Natl. Acad. Sci. USA* **104**, 18157-18162.

Emery, A. E. (2002). The muscular dystrophies. *Lancet* **359**, 687-695.

Engel, W. K. and Kossman, R. J. (1963). Selective involvement of histochemical type I muscle fibers in a patient with facioscapulohumeral muscular dystrophy. *Neurology (Minneapolis)* **13**, 362.

Fenichel, G. M., Emery, E. S. and Hunt, P. (1967). Neurogenic atrophy simulating facioscapulohumeral dystrophy. A dominant form. *Arch. Neurol.* **17**, 257-260.

Furukawa, T., Tsukagoshi, H., Sugita, H. and Toyokura, Y. (1969). Neurogenic muscular atrophy simulating facioscapulohumeral muscular dystrophy with particular reference to the heterogeneity of Kugelberg-Welander disease. *J. Neurol. Sci.* **9**, 389-397.

Gabellini, D., Green, M. R. and Tupler, R. (2002). Inappropriate gene activation in FSHD: a repressor complex binds a chromosomal repeat deleted in dystrophic muscle. *Cell* **110**, 339-348.

Gabellini, D., D'Antona, G., Moggio, M., Prelle, A., Zecca, C., Adami, R., Angeletti, B., Ciscato, P., Pellegrino, M. A., Bottinelli, R. et al. (2006). Facioscapulohumeral muscular dystrophy in mice overexpressing FRG1. *Nature* **439**, 973-977.

Gabriëls, J., Beckers, M. C., Ding, H., De Vriese, A., Plaisance, S., van der Maarel, S. M., Padberg, G. W., Frants, R. R., Hewitt, J. E., Collen, D. et al. (1999). Nucleotide sequence of the partially deleted D4Z4 locus in a patient with FSHD identifies a putative gene within each 3.3 kb element. *Gene* **236**, 25-32.

Ghersa, P., Gobert, R. P., Sattonnet-Roche, P., Richards, C. A., Merlo Pich, E. and Hooft van Huijsduijnen, R. (1998). Highly controlled gene expression using combinations of a tissue-specific promoter, recombinant adenovirus and a tetracycline-regulatable transcription factor. *Gene Ther.* **5**, 1213-1220.

Gurnett, C. A., Alaee, F., Kruse, L. M., Desruisseau, D. M., Hecht, J. T., Wise, C. A., Bowcock, A. M. and Dobbs, M. B. (2008). Asymmetric lower-limb malformations in individuals with homeobox PITX1 gene mutation. *Am. J. Hum. Genet.* **83**, 616-622.

Hudgson, P., Bradley, W. G. and Jenkison, M. (1972). Familial "mitochondrial" myopathy: a myopathy associated with disordered oxidative metabolism in muscle fibres. Part 1. Clinical, electrophysiological and pathological findings. *J. Neurol. Sci.* **16**, 343-370.

Jackman, R. W. and Kandarian, S. C. (2004). The molecular basis of skeletal muscle atrophy. *Am. J. Physiol. Cell Physiol.* **287**, C834-C843.

Jagoe, R. T., Lecker, S. H., Gomes, M. and Goldberg, A. L. (2002). Patterns of gene expression in atrophying skeletal muscles: response to food deprivation. *FASEB J.* **16**, 1697-1712.

Jiang, G., Yang, F., van Overveld, P. G., Vedanarayanan, V., van der Maarel, S. and Ehrlich, M. (2003). Testing the position-effect variegation hypothesis for facioscapulohumeral muscular dystrophy by analysis of histone modification and gene expression in subtelomeric 4q. *Hum. Mol. Genet.* **12**, 2909-2921.

Kilmer, D. D., Abresch, R. T., McCrory, M. A., Carter, G. T., Fowler, W. M., Jr, Johnson, E. R. and McDonald, C. M. (1995). Profiles of neuromuscular diseases: facioscapulohumeral muscular dystrophy. *Am. J. Phys. Med. Rehabil.* **74 Suppl,** S131-S139.

Kioussi, C., Briata, P., Baek, S. H., Rose, D. W., Hamblet, N. S., Herman, T., Ohgi, K. A., Lin, C., Gleiberman, A., Wang, J. et al. (2002). Identification of a Wnt/Dvl/beta-Catenin --> Pitx2 pathway mediating cell-type-specific proliferation during development. *Cell* **111**, 673-685.

Kissel, J. T. (1999). Facioscapulohumeral dystrophy. *Semin. Neurol.* **19**, 35-43.

Kolfschoten, I. G., van Leeuwen, B., Berns, K., Mullenders, J., Beijersbergen, R. L., Bernards, R., Voorhoeve, P. M. and Agami, R. (2005). A genetic screen identifies PITX1 as a suppressor of RAS activity and tumorigenicity. *Cell* **121**, 849-858.

Kowaljow, V., Marcowycz, A., Ansseau, E., Conde, C. B., Sauvage, S., Mattéotti, C., Arias, C., Corona, E. D., Nuñez, N. G., Leo, O. et al. (2007). The DUX4 gene at the FSHD1A locus encodes a pro-apoptotic protein. *Neuromuscul. Disord.* **17**, 611-623.

L'Honoré, A., Coulon, V., Marcil, A., Lebel, M., Lafrance-Vanasse, J., Gage, P., Camper, S. and Drouin, J. (2007). Sequential expression and redundancy of Pitx2 and Pitx3 genes during muscle development. *Dev. Biol.* **307**, 421-433.

L'Honoré, A., Ouimette, J.-F., Lavertu-Jolin, M. and Drouin, J. (2010). Pitx2 defines alternate pathways acting through MyoD during limb and somitic myogenesis. *Development* **137**, 3847-3856.

Lamba, P., Khivansara, V., D'Alessio, A. C., Santos, M. M. and Bernard, D. J. (2008). Paired-like homeodomain transcription factors 1 and 2 regulate follicle-stimulating hormone beta-subunit transcription through a conserved cis-element. *Endocrinology* **149**, 3095-3108.

Lamonerie, T., Tremblay, J. J., Lanctôt, C., Therrien, M., Gauthier, Y. and Drouin, J. (1996). Ptx1, a bicoid-related homeo box transcription factor involved in transcription of the pro-opiomelanocortin gene. *Genes Dev.* **10**, 1284-1295.

Lanctôt, C., Moreau, A., Chamberland, M., Tremblay, M. L. and Drouin, J. (1999). Hindlimb patterning and mandible development require the Ptx1 gene. *Development* **126**, 1805-1810.

Laoudj-Chenivesse, D., Carnac, G., Bisbal, C., Hugon, G., Bouillot, S., Desnuelle, C., Vassetzky, Y. and Fernandez, A. (2005). Increased levels of adenine nucleotide translocator 1 protein and response to oxidative stress are early events in facioscapulohumeral muscular dystrophy muscle. *J. Mol. Med.* **83**, 216-224.

Lemmers, R. J. L. F., van der Vliet, P. J., Klooster, R., Sacconi, S., Camaño, P., Dauwerse, J. G., Snider, L., Straasheijm, K. R., van Ommen, G. J., Padberg, G. W. et al. (2010). A unifying genetic model for facioscapulohumeral muscular dystrophy. *Science* **329**, 1650-1653.

Leucht, P., Kim, J. B., Amasha, R., James, A. W., Girod, S. and Helms, J. A. (2008). Embryonic origin and Hox status determine progenitor cell fate during adult bone regeneration. *Development* **135**, 2845-2854.

Lin, M. Y. and Nonaka, I. (1991). Facioscapulohumeral muscular dystrophy: muscle fiber type analysis with particular reference to small angular fibers. *Brain Dev.* **13**, 331-338.

Liu, D. X. and Lobie, P. E. (2007). Transcriptional activation of p53 by Pitx1. *Cell Death Differ.* **14**, 1893-1907.

Logan, M. and Tabin, C. J. (1999). Role of Pitx1 upstream of Tbx4 in specification of hindlimb identity. *Science* **283**, 1736-1739.

Lunt, P. W. and Harper, P. S. (1991). Genetic counselling in facioscapulohumeral muscular dystrophy. *J. Med. Genet.* **28**, 655-664.

Mammucari, C., Milan, G., Romanello, V., Masiero, E., Rudolf, R., Del Piccolo, P., Burden, S. J., Di Lisi, R., Sandri, C., Zhao, J. et al. (2007). FoxO3 controls autophagy in skeletal muscle in vivo. *Cell Metab.* **6**, 458-471.

Marcil, A., Dumontier, E., Chamberland, M., Camper, S. A. and Drouin, J. (2003). Pitx1 and Pitx2 are required for development of hindlimb buds. *Development* **130**, 45-55.

Masny, P. S., Bengtsson, U., Chung, S. A., Martin, J. H., van Engelen, B., van der Maarel, S. M. and Winokur, S. T. (2004). Localization of 4q35.2 to the nuclear periphery: is FSHD a nuclear envelope disease? *Hum. Mol. Genet.* **13**, 1857-1871.

Matecki, S., Guibinga, G. H. and Petrof, B. J. (2004). Regenerative capacity of the dystrophic (mdx) diaphragm after induced injury. *Am. J. Physiol. Regul. Integr. Comp. Physiol.* **287**, R961-R968.

Moresi, V., Pristerà, A., Scicchitano, B. M., Molinaro, M., Teodori, L., Sassoon, D., Adamo, S. and Coletti, D. (2008). Tumor necrosis factor-alpha inhibition of skeletal muscle regeneration is mediated by a caspase-dependent stem cell response. *Stem Cells* **26**, 997-1008.

Nakagawa, M., Matsuzaki, T., Higuchi, I., Fukunaga, H., Inui, T., Nagamitsu, S., Yamada, H., Arimura, K. and Osame, M. (1997). Facioscapulohumeral muscular dystrophy: clinical diversity and genetic abnormalities in Japanese patients. *Intern. Med.* **36**, 333-339.

Neudecker, S., Krasnianski, M., Bahn, E. and Zierz, S. (2004). Rimmed vacuoles in facioscapulohumeral muscular dystrophy: a unique ultrastructural feature. *Acta Neuropathol.* **108**, 257-259.

Olsen, D. B., Gideon, P., Jeppesen, T. D. and Vissing, J. (2006). Leg muscle involvement in facioscapulohumeral muscular dystrophy assessed by MRI. *J. Neurol.* **253**, 1437-1441.

Padberg, G. W., Lunt, P. W., Koch, M. and Fardeau, M. (1991). Diagnostic criteria for facioscapulohumeral muscular dystrophy. *Neuromuscul. Disord.* **1**, 231-234.

Padberg, G. W., Frants, R. R., Brouwer, O. F., Wijmenga, C., Bakker, E. and Sandkuijl, L. A. (1995a). Facioscapulohumeral muscular dystrophy in the Dutch population. *Muscle Nerve* **18 S13**, S81-S84.

Padberg, G. W., Brouwer, O. F., de Keizer, R. J., Dijkman, G., Wijmenga, C., Grote, J. J. and Frants, R. R. (1995b). On the significance of retinal vascular disease and hearing loss in facioscapulohumeral muscular dystrophy. *Muscle Nerve* **18 S13**, S73-S80.

Pallafacchina, G., Calabria, E., Serrano, A. L., Kalhovde, J. M. and Schiaffino, S. (2002). A protein kinase B-dependent and rapamycin-sensitive pathway controls skeletal muscle growth but not fiber type specification. *Proc. Natl. Acad. Sci. USA* **99**, 9213-9218.

Porrello, A., Cerone, M. A., Coen, S., Gurtner, A., Fontemaggi, G., Cimino, L., Piaggio, G., Sacchi, A. and Soddu, S. (2000). p53 regulates myogenesis by triggering the differentiation activity of pRb. *J. Cell Biol.* **151**, 1295-1304.

Qi, D.-L., Ohhira, T., Fujisaki, C., Inoue, T., Ohta, T., Osaki, M., Ohshiro, E., Seko, T., Aoki, S., Oshimura, M. et al. (2011). Identification of PITX1 as a TERT suppressor gene located on human chromosome 5. *Mol. Cell. Biol.* **31**, 1624-1636.

Qureshi, A. R., Alvestrand, A., Danielsson, A., Divino-Filho, J. C., Gutierrez, A., Lindholm, B. and Bergström, J. (1998). Factors predicting malnutrition in hemodialysis patients: a cross-sectional study. *Kidney Int.* **53**, 773-782.

Reilich, P., Schramm, N., Schoser, B., Schneiderat, P., Strigl-Pill, N., Müller-Höcker, J., Kress, W., Ferbert, A., Rudnik-Schöneborn, S., Noth, J. et al. (2010). Facioscapulohumeral muscular dystrophy presenting with unusual phenotypes and atypical morphological features of vacuolar myopathy. *J. Neurol.* **257**, 1108-1118.

Rinn, J. L., Wang, J. K., Allen, N., Brugmann, S. A., Mikels, A. J., Liu, H., Ridky, T. W., Stadler, H. S., Nusse, R., Helms, J. A. et al. (2008). A dermal HOX transcriptional program regulates site-specific epidermal fate. *Genes Dev.* **22**, 303-307.

Sandri, M., El Meslemani, A. H., Sandri, C., Schjerling, P., Vissing, K., Andersen, J. L., Rossini, K., Carraro, U. and Angelini, C. (2001). Caspase 3 expression correlates with skeletal muscle apoptosis in Duchenne and facioscapulo human muscular dystrophy. A potential target for pharmacological treatment? *J. Neuropathol. Exp. Neurol.* **60**, 302-312.

Schwarzkopf, M., Coletti, D., Sassoon, D. and Marazzi, G. (2006). Muscle cachexia is regulated by a p53-PW1/Peg3-dependent pathway. *Genes Dev.* **20**, 3440-3452.

Shapiro, M. D., Marks, M. E., Peichel, C. L., Blackman, B. K., Nereng, K. S., Jónsson, B., Schluter, D. and Kingsley, D. M. (2004). Genetic and developmental basis of evolutionary pelvic reduction in threespine sticklebacks. *Nature* **428**, 717-723.

Shih, H. P., Gross, M. K. and Kioussi, C. (2007). Expression pattern of the homeodomain transcription factor Pitx2 during muscle development. *Gene Expr. Patterns* **7**, 441-451.

Singh, D., Febbo, P. G., Ross, K., Jackson, D. G., Manola, J., Ladd, C., Tamayo, P., Renshaw, A. A., D'Amico, A. V., Richie, J. P. et al. (2002). Gene expression correlates of clinical prostate cancer behavior. *Cancer Cell* **1**, 203-209.

Slipetz, D. M., Aprille, J. R., Goodyer, P. R. and Rozen, R. (1991). Deficiency of complex III of the mitochondrial respiratory chain in a patient with facioscapulohumeral disease. *Am. J. Hum. Genet.* **48**, 502-510.

Soddu, S., Blandino, G., Scardigli, R., Coen, S., Marchetti, A., Rizzo, M. G., Bossi, G., Cimino, L., Crescenzi, M. and Sacchi, A. (1996). Interference with p53 protein inhibits hematopoietic and muscle differentiation. *J. Cell Biol.* **134**, 193-204.

St Amand, T. R., Zhang, Y., Semina, E. V., Zhao, X., Hu, Y., Nguyen, L., Murray, J. C. and Chen, Y. (2000). Antagonistic signals between BMP4 and FGF8 define the expression of Pitx1 and Pitx2 in mouse tooth-forming anlage. *Dev. Biol.* **217**, 323-332.

Subramanian, L., Crabb, J. W., Cox, J., Durussel, I., Walker, T. M., van Ginkel, P. R., Bhattacharya, S., Dellaria, J. M., Palczewski, K. and Polans, A. S. (2004). Ca2+ binding to EF hands 1 and 3 is essential for the interaction of apoptosis-linked gene-2 with Alix/AIP1 in ocular melanoma. *Biochemistry* **43**, 11175-11186.

Szeto, D. P., Rodriguez-Esteban, C., Ryan, A. K., O'Connell, S. M., Liu, F., Kioussi, C., Gleiberman, A. S., Izpisúa-Belmonte, J. C. and Rosenfeld, M. G. (1999). Role of the Bicoid-related homeodomain factor Pitx1 in specifying hindlimb morphogenesis and pituitary development. *Genes Dev.* **13**, 484-494.

Tamir, Y. and Bengal, E. (1998). p53 protein is activated during muscle differentiation and participates with MyoD in the transcription of muscle creatine kinase gene. *Oncogene* **17**, 347-356.

Tawil, R. and Van Der Maarel, S. M. (2006). Facioscapulohumeral muscular dystrophy. *Muscle Nerve* **34**, 1-15.

Tawil, R., Figlewicz, D. A., Griggs, R. C. and Weiffenbach, B. (1998). Facioscapulohumeral dystrophy: a distinct regional myopathy with a novel molecular pathogenesis. *Ann. Neurol.* **43**, 279-282.

Taylor, D. A., Carroll, J. E., Smith, M. E., Johnson, M. O., Johnston, G. P. and Brooke, M. H. (1982). Facioscapulohumeral dystrophy associated with hearing loss and Coats syndrome. *Ann. Neurol.* **12**, 395-398.

Tisdale, M. J. (1997). Biology of cachexia. *J. Natl. Cancer Inst.* **89**, 1763-1773.

Tremblay, J. J., Lanctôt, C. and Drouin, J. (1998). The pan-pituitary activator of transcription, Ptx1 (pituitary homeobox 1), acts in synergy with SF-1 and Pit1 and is an upstream regulator of the Lim-homeodomain gene Lim3/Lhx3. *Mol. Endocrinol.* **12**, 428-441.

Tsumagari, K., Chang, S.-C., Lacey, M., Baribault, C., Chittur, S. V., Sowden, J., Tawil, R., Crawford, G. E. and Ehrlich, M. (2011). Gene expression during normal and FSHD myogenesis. *BMC Med. Genomics* **4**, 67.

Tyler, F. H. and Stephens, F. E. (1950). Studies in disorders of muscle. II Clinical manifestations and inheritance of facioscapulohumeral dystrophy in a large family. *Ann. Intern. Med.* **32**, 640-660.

Tyner, S. D., Venkatachalam, S., Choi, J., Jones, S., Ghebranious, N., Igelmann, H., Lu, X., Soron, G., Cooper, B., Brayton, C. et al. (2002). p53 mutant mice that display early ageing-associated phenotypes. *Nature* **415**, 45-53.

van Deutekom, J. C. T., Wijmenga, C., van Tienhoven, E. A. E., Gruter, A.-M., Hewitt, J. E., Padberg, G. W., van Ommen, G.-J. B., Hofker, M. H. and Frants, R. R. (1993). FSHD associated DNA rearrangements are due to deletions of integral copies of a 3.2 kb tandemly repeated unit. *Hum. Mol. Genet.* **2**, 2037-2042.

van Overveld, P. G., Lemmers, R. J., Sandkuijl, L. A., Enthoven, L., Winokur, S. T., Bakels, F., Padberg, G. W., van Ommen, G. J., Frants, R. R. and van der Maarel, S. M. (2003). Hypomethylation of D4Z4 in 4q-linked and non-4q-linked facioscapulohumeral muscular dystrophy. *Nat. Genet.* **35**, 315-317.

Vanderplanck, C., Ansseau, E., Charron, S., Stricwant, N., Tassin, A., Laoudj-Chenivesse, D., Wilton, S. D., Coppée, F. and Belayew, A. (2011). The FSHD atrophic myotube phenotype is caused by DUX4 expression. *PLoS ONE* **6**, e26820.

Voit, T., Lamprecht, A., Lenard, H. G. and Goebel, H. H. (1986). Hearing loss in facioscapulohumeral dystrophy. *Eur. J. Pediatr.* **145**, 280-285.

Vousden, K. H. (2000). p53: death star. *Cell* **103**, 691-694.

Wallace, L. M., Garwick, S. E., Mei, W., Belayew, A., Coppee, F., Ladner, K. J., Guttridge, D., Yang, J. and Harper, S. Q. (2011). DUX4, a candidate gene for facioscapulohumeral muscular dystrophy, causes p53-dependent myopathy in vivo. *Ann. Neurol.* **69**, 540-552.

Wegel, E. and Shaw, P. (2005). Gene activation and deactivation related changes in the three-dimensional structure of chromatin. *Chromosoma* **114**, 331-337.

Weissman, J. R., Kelley, R. I., Bauman, M. L., Cohen, B. H., Murray, K. F., Mitchell, R. L., Kern, R. L. and Natowicz, M. R. (2008). Mitochondrial disease in autism spectrum disorder patients: a cohort analysis. *PLoS ONE* **3**, e3815.

Winokur, S. T., Barrett, K., Martin, J. H., Forrester, J. R., Simon, M., Tawil, R., Chung, S. A., Masny, P. S. and Figlewicz, D. A. (2003). Facioscapulohumeral muscular dystrophy (FSHD) myoblasts demonstrate increased susceptibility to oxidative stress. *Neuromuscul. Disord.* **13**, 322-333.

Yamaguchi, T., Miki, Y. and Yoshida, K. (2010). The c-Abl tyrosine kinase stabilizes Pitx1 in the apoptotic response to DNA damage. *Apoptosis* **15**, 927-935.

Yoshioka, H., Meno, C., Koshiba, K., Sugihara, M., Itoh, H., Ishimaru, Y., Inoue, T., Ohuchi, H., Semina, E. V., Murray, J. C. et al. (1998). Pitx2, a bicoid-type homeobox gene, is involved in a lefty-signaling pathway in determination of left-right asymmetry. *Cell* **94**, 299-305.

Zacharias, A. L., Lewandoski, M., Rudnicki, M. A. and Gage, P. J. (2011). Pitx2 is an upstream activator of extraocular myogenesis and survival. *Dev. Biol.* **349**, 395-405.

Zeng, W., de Greef, J. C., Chen, Y. Y., Chien, R., Kong, X., Gregson, H. C., Winokur, S. T., Pyle, A., Robertson, K. D., Schmiesing, J. A. et al. (2009). Specific loss of histone H3 lysine 9 trimethylation and HP1gamma/cohesin binding at D4Z4 repeats is associated with facioscapulohumeral dystrophy (FSHD). *PLoS Genet.* **5**, e1000559.